November 19, 2012
TPF-5(264)
Task 3 Preliminary Field Test Report

TAST 3A REPORT

PASSIVE FORCE-DEFLECTION TESTS FOR SKEWED ABUTMENTS WITH TRANSVERSE WINGWALLS

Prepared By

Kyle M. Rollins, Professor, Civil & Env. Engrg Dept., Brigham Young Univ., 368 CB, Provo, UT 84602, (801) 422-6334, rollinsk@byu.edu

Aaron K. Marsh, Research Asst., Civil & Env. Engrg Dept., Brigham Young Univ., 368 CB, Provo, UT 84602, (801) 341-9651; aaron.kirt@gmail.com

Bryan Franke, Research Asst., Civil & Env. Engrg Dept., Brigham Young Univ., 368 CB, Provo, UT 84602, bryan.franke@gmail.com

Jaycee Smith, Research Asst., Civil & Env. Engrg Dept., Brigham Young Univ., 368 CB, Provo, UT 84602, jayceeofsocal@gmail.com

Katie Palmer, Research Asst., Civil & Env. Engrg Dept., Brigham Young Univ., 368 CB, Provo, UT 84602, katienpalmer@gmail.com

Prepared for

Research Division of the Utah Department of Transportation

November 19, 2012

EXECUTIVE SUMMARY

Accounting for seismic forces and thermal expansion in bridge design requires an accurate passive force-deflection relationship for the abutment wall. Current design codes make no allowance for skew effects on passive force; however, quarter scale lab tests indicate that there is a significant reduction in peak passive force as skew angle increases for plane-strain cases. To further explore this issue larger scale field tests were conducted with skew angles of 0°, 15°, and 30° with transverse wingwalls. The abutment backwall was 11-ft (3.35-m) wide by 5.5-ft (1.68-m) high and backfill material consisted of dense compacted sand. The peak passive force for the 15° and 30° skew tests was found to be 72% and 57%, respectively of the peak passive force for the 0° skew case. These results are in good agreement with the available laboratory and numerical results; however, discrepancies may suggest that backfill geometry has some effect on the reduction in peak passive force with respect to skew angle. Longitudinal displacement of the backwall at the peak passive force was found to be between 3% and 4.5% of the backwall height for the 0°, 15°, and 30° skew tests which is consistent with previously reported values for large-scale passive force-deflection tests. Passive pressure across the backwall was initially uniform but showed became non-uniform at larger displacements with the highest values at the obtuse corner. Shear force on the backwall increased as skew angle increased despite the reduction in longitudinal force with skew angle. Transverse pile cap displacement also increased with skew angle and were sufficient to mobilize the frictional resistance. Heave geometries for the 0°, 15°, and 30° tests were quite typically 3% to 4% of the fill height. In all cases the failure geometry extended approximately 4 ft to 5 ft (1.22 m to 1.52 m) beyond the edge of the pile cap and 16 ft (4.88 m) from the face of the cap when measured perpendicular to the backwall.

INTRODUCTION

Numerous large-scale experiments have been conducted with the intent to determine the passive force-deflection curves that might be expected for dense compacted fill behind non-skewed bridge abutments (Mokwa and Duncan 2001; Rollins and Cole 2006; Rollins et al. 2010; Rollins and Sparks 2002). Much of this research indicates that the peak passive force can be accurately predicted using the log-spiral method and is achieved at a longitudinal deflection of 3% to 5% of the backwall height (Rollins and Cole 2006). Methods approximating the complete passive force-deflection curve with a hyperbola have been developed by Shamsabadi et al. (2007) and Duncan and Mokwa (2001). However, for simplicity in design, most specifications recommend a bilinear relationship (AASHTO 2011; Caltrans 2001).

Until recently, no large-scale experiments had been conducted to determine the passive force-deflection relationships for skewed bridge abutments. Furthermore, current bridge design practices assume the peak passive force is the same for skewed bridges as for non-skewed bridges (AASHTO 2011). However, field evidence clearly indicates poorer performance of skewed abutments during seismic events (Apirakyorapinit et al. 2012; Elnashai et al. 2010; Shamsabadi et al. 2006; Unjohn 2012) and distress to skewed abutments due to thermal expansion (Steinberg and Sargand 2010). Laboratory tests performed by Rollins and Jessee (2012) and numerical analyses performed reported by Shamsabadi et al. (2006) both found that there is a significant reduction in passive force as skew angle increases. Using data obtained from these studies, Rollins and Jessee (2012) proposed the correction factor, R_{skew}, given by Equation (1) which defines the ratio between the peak passive force for a skewed abutment ($P_{P\text{-}skew}$) and the peak passive force for a non-skewed abutment ($P_{P\text{-}no\ skew}$) as a function of skew angle, θ.

$$R_{skew} = P_{P-skew} / P_{P-no\ skew} = 8.0 * 10^{-5}\theta^2 - 0.018\theta + 1.0 \quad (1)$$

To more fully understand the relationship between skew angle and reduction in peak passive force, two large-scale tests were conducted to determine the passive force-deflection curves for skew angles of 0° and 30°. These tests were conducted using an existing 11-ft (3.35-m) wide by 5.5-ft (1.68-m)

high by 15-ft (4.57-m) long pile cap which has been used for a number of previously conducted lateral load and passive force-deflection tests (Rollins et al. 2010; Rollins and Sparks 2002; Strassburg 2010). The 0° skew test for this study was conducted in a similar fashion to the tests conducted by the previous researchers. For the 15° and 30° skew tests a concrete wedge was attached to the face of the existing pile cap. Testing procedures, results, comparisons to available results and recommendations based on analysis of the test results are presented in this paper.

BACKGROUND

As outlined by Burke Jr. (1994) and shown in Figure 1, the interaction of forces at the interface between the bridge abutment backwall and soil backfill may be expressed in terms of the total longitudinal force, P_L, and its components normal to and transverse to the abutment. The normal force is resisted by the passive force, P_P [see Equation (2)]; and the transverse, or shear force, P_T [see Equation (3)], is resisted by the shear resistance, P_R [see Equation (4)]. To prevent instability of the bridge caused by sliding of the abutment against the soil backfill the inequality shown in Equation (5) must be satisfied. In addition, rotation of the entire bridge can occur if the inequality in Equation (6) is not satisfied.

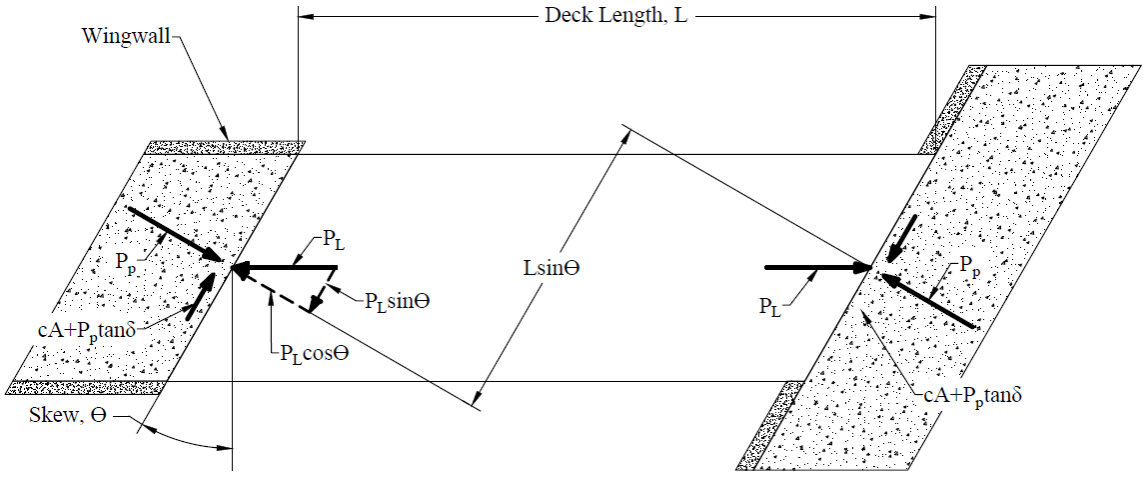

FIGURE 1 Typical distribution of forces on a bridge with skewed abutments.

$$P_P = P_L \cos\theta \tag{2}$$

$$P_T = P_L \sin\theta \tag{3}$$

$$P_R = cA + P_P \tan\delta \tag{4}$$

$$\frac{cA + P_P \tan\delta}{F_s} \geq P_L \sin\theta \tag{5}$$

$$\frac{cA + P_P \tan\delta \;\; L\cos\theta}{F_s} \geq P_P L \sin\theta \tag{6}$$

where

θ = skew angle of backwall

c = soil cohesion

A = backwall area

δ = angle of friction between backfill soil and abutment wall

F_s = factor of safety

L = length of bridge

These equations are only strictly valid if the bridge remains stable; therefore, if the bridge rotates, the distribution of forces on the abutment backwall will likely change, rendering these equations less accurate. Based on Equation (6), Burke Jr. (1994) noted that if cohesion is ignored the potential for bridge rotation is independent of passive force and bridge length so that at a typical design interface friction angle of 22°, the factor of safety decreases to below 1.5 if bridge skew exceeds 15°.

TEST CONFIGURATION

Test Geometry

The test setup for the lab tests is shown in Figure 2 and involved a 2 ft (0.61 m) high by 4 ft (1.22 m) wide backwall with a 2D or plane-strain backfill geometry (Rollins and Jessee 2012). In contrast, the field tests used an existing 11 ft (3.35 m) wide by 5.5 ft (1.68 m) high by 15 ft (4.57 m) long pile cap to simulate an abutment backwall as shown in Figure 3. Instead of a 2D backfill geometry, the backfill was placed in a test pit that extended a little over 5 ft (1.52 m) out from the sides of the pile cap to the edge of the test pit with transverse concrete wingwalls to allow for the development of a 3D failure geometry. The

backfill extended 24 ft (7.32 m) longitudinally from the face of the pile cap and approximately 1 ft (0.30 m) below the bottom of the cap from the face to 10 ft (3.05 m) from the face to contain the potential failure surface. Though the native soil was significantly stiffer than the backfill materials, the backfill boundaries were considered to be far enough away to not affect the development of a shear surface. Beyond 10 ft (3.05 m), the base of the backfill tapered up to be approximately even with the base of the cap to reduce the required backfill volume.

Load was applied in the longitudinal direction with two 600-kip (2,670 kN) hydraulic actuators which reacted against a sheet pile wall and two 4-ft (1.22 m) diameter drilled shafts that were coupled together by two deep beams.

After conducting the test for the 0° skew conditions, 15° and 30° wedges were attached to the front face of the pile cap for subsequent skew tests as shown in Figure 3. Rollers were placed beneath the wedge to eliminate base friction resistance.

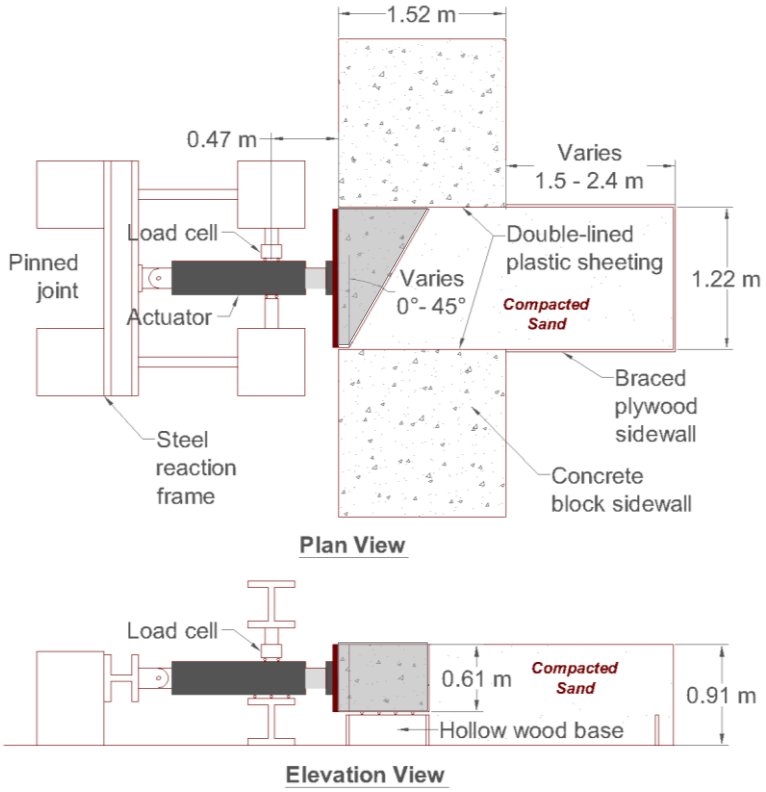

FIGURE 2 Schematic drawings of lab test layout (Rollins and Jessee 2012) (NOTE 1 m = 3.281 ft).

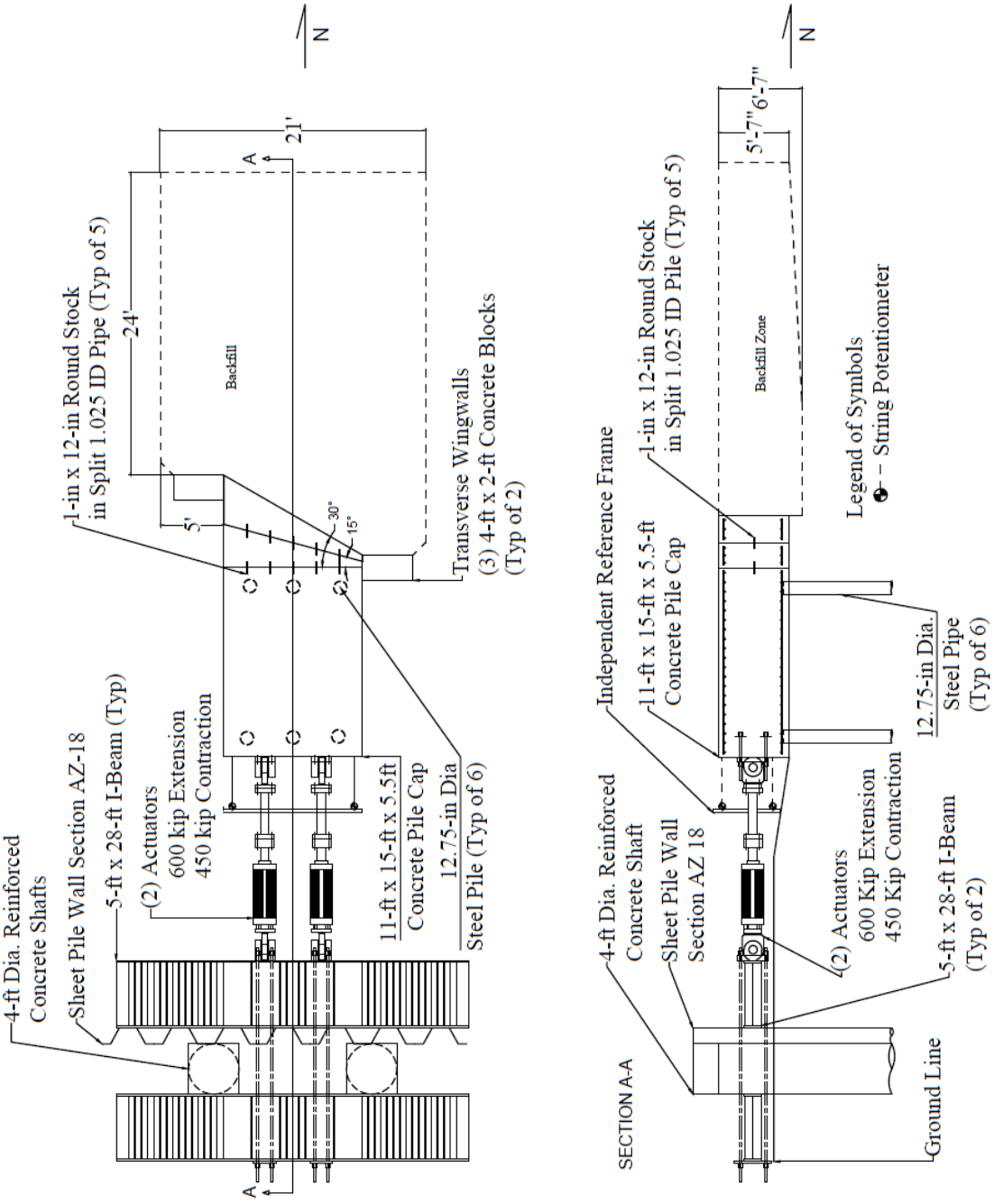

FIGURE 3 Schematic drawings of field test layout (NOTE 1 ft = 0.305 m).

Instrumentation

Longitudinal load was measured using pressure transducers in the actuators. Longitudinal displacement of the pile cap was measured using four string potentiometers (string pots) located at each corner of the back of the pile cap and were tied to an independent reference frame. As the piles were assumed to provide vertical restraint, vertical movement of the pile cap was not monitored. Longitudinal and transverse deflection versus displacements data profiles were measured using inclinometers and shape accelerometer arrays which extended approximately 40 ft (14 m) into the center pile in the North and South sides of the pile cap. The shape arrays provided data at 1 ft (0.30 m) intervals while the inclinometers provided data at 2 ft (0.6 m) intervals. Because of the time required to obtain inclinometer readings, the inclinometer measurements were only taken immediately before the start of a test and after the last deflection increment. In contrast, the shape arrays provided profiles at each deflection increment because their collection was instantaneous.

For the 30º skew test only a total of six "Fat Back" pressure cells manufactured by Geokon® were installed horizontally across the face of the skew wedge as shown in Figure 4. These pressure cells defined the horizontal pressure distribution at the interface with the soil as the pile cap was pushed into the backfill soil. Unfortunately, pressure plate PP1498 failed to function properly during the first test due to difficulties while removing the concrete forms. However, the remaining five pressure plates still functioned properly and produced sufficient data to understand the pressure distribution characteristics across the entire interface.

To measure backfill heave a 2 ft (0.61 m) grid was painted on the backfill surface and the relative elevation of each grid intersection was measured with a survey level prior to, and after conducting each test. Surface cracks in the backfill were also marked following the completion of each test. A hand auger was used to drill 2-in (51-mm) diameter, vertical holes at various locations through the backfill in order to determine the location of the internal failure surfaces. These holes were then refilled and compacted with red-dyed sand.

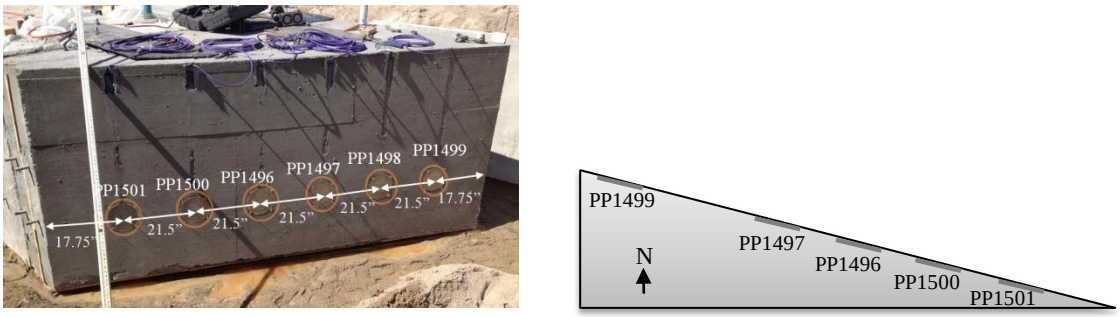

[A] [B]

FIGURE 4 [A] Pile cap wedge interface. [B] Plan view drawing of pressure plates.

Following final pile cap displacement, a trench was excavated adjacent to these holes and the offset in the sand columns identified the locations of the failure surfaces. For the 0° test, sand columns were located on the longitudinal centerline at 2, 4, 6, and 8 ft (0.61, 1.22, 1.83, and 2.44 m) from the backwall face. For the 30° test, sand columns were located 2 ft (0.61 m) on each side of the longitudinal center line, at distances of 2, 6, 10, 14, and 18 ft (0.61, 1.83, 3.05, 4.27, and 5.49 m) from the face of the backwall. For the 15° test, sand columns were located 4 ft (1.22 m) on each side of a line running perpendicular to the center of the wall face at distances of 2, 6, and 9 ft (0.61, 1.83, and 2.74 m) from the face of the backwall.

Geotechnical Backfill Properties

Backfill materials consisted of a poorly-graded sand (SP or A-1-b as classified by the Unified Soil Classification System or AASHTO classification system, respectively). The particle-size distribution generally falls within the gradation limits for washed concrete sand (ASTM C33) as shown in Figure 5. Gradations before and after the test series found that the coefficient of uniformity (C_u) and coefficient of curvature (C_c) were 7.6 and 0.8 pre-test, and 9.7 and 0.7 post-test, respectively. This variability is likely

due to small differences in soil samples. For comparison, the C_u and C_c values from the lab tests were 3.7 and 0.7, respectively. Figure 5 also shows the soil gradation for the lab tests.

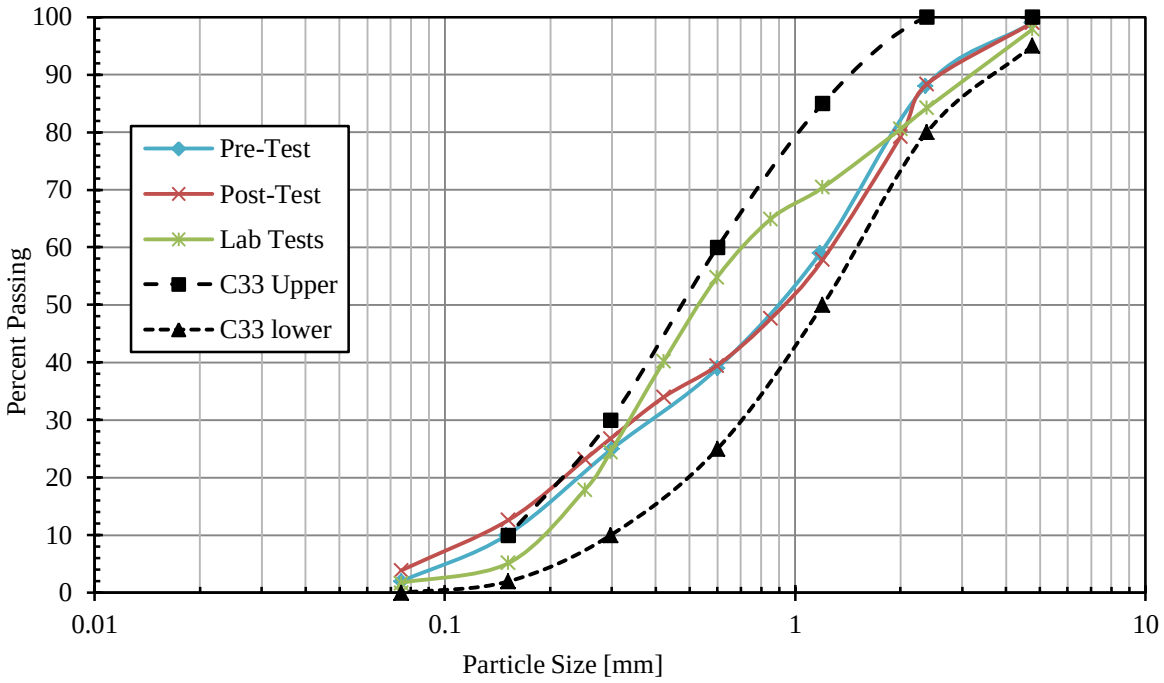

FIGURE 5 Gradation for backfill sand relative to concrete sand gradation.

Unit Weight and Moisture Content

Maximum dry unit weight according to the modified Proctor compaction test (ASTM D1557) performed prior to testing was 111.5 lbf/ft^3 (17.52 kN/m^3) and the optimum moisture content was 7.1%. The target on-site compaction level was 95% of the modified Proctor maximum. Backfill sand was placed in lifts approximately 6-in (15.24-cm) thick and compacted with a smooth-drum vibratory roller and a walk-behind vibratory plate compactor to an average density greater than approximately 95% of the modified Proctor maximum. A nuclear density gauge was used to obtain relative compaction and water content data during compaction. Though not shown, the variation of relative compaction and moisture content with depth was not significant. Relative density was estimated using the empirical relationship

between relative density (D_r) and relative compaction (R) for granular materials developed by Lee and Singh (1971) as shown in Equation (7) where D_r and R are measured in percent.

$$R = 80 + 0.2D_r \quad (7)$$

A summary of the soil density and water content measurements for the three tests is shown in Table 1. The properties of the two backfills were generally very consistent. Average relative compaction, relative density, and water content for the three tests were 96.8%, 84%, 8.9%, respectively. For comparison purposes the average relative compaction, relative density, and water content for the laboratory tests were 97.9%, 90%, and 8.0%, respectively (Rollins and Jessee 2012).

TABLE 1 Summary of Compaction and Water Content Data for Each Test

Backfill Soil Properties	**0° Skew Test**	**15° Skew Test**	**30° Skew Test**
Minimum Dry Unit Weight [pcf]	105.4	106.3	105.6
Maximum Dry Unit Weight [pcf]	109.9	110.5	110.1
Average Dry Unit Weight [pcf]	107.0	108.3	108.3
Relative Compaction	96.0%	97.2%	97.2%
Relative Density	80.0%	86.0%	86.0%
Moisture Content	8.9%	9.5%	8.3%

Shear Strength

Direct shear tests were conducted at the field density and moisture content values, and the drained friction angle (ϕ') was found to be 41° with a cohesion of 96 lbs/ft^2 (4.61 kN/m^2). Previous researchers (Rollins and Cole 2006; Rollins and Jessee 2012) conducted direct shear tests and determined that the interface friction angle (δ) between similar sand and concrete was about 75% of the soil friction angle. For comparison purposes, the drained friction angle of the sand for the laboratory skew tests was 46° with a cohesion of 70 lbs/ft^2 (3.35 kPa) (Rollins and Jessee 2012).

General Test Procedures

Prior to testing with the backfill in place, a lateral load test was performed to determine the "baseline" resistance of the pile cap alone, and the pile cap with attached wedge. Because the pile cap had been previously employed for a number of tests, the baseline resistance has become relatively linear.

Following the baseline test, backfill was compacted adjacent to the cap and a lateral load test was performed to obtain the total resistance. Following backfill compaction, the grid and soil columns were installed and appropriate initial measurements, including relative elevations of the grid points, were recorded. The backfill material was completely excavated and recompacted for each individual test.

The pile cap (and attached wedge if applicable) was then pushed longitudinally into the backfill zone in 0.25-in (6.35-mm) increments at a velocity of 0.25 in/min (6.35 mm/min) to a final displacement of 3.25 in to 3.75 in (8.30 cm to 9.53 cm) using the two hydraulic actuators. At each 0.25-in (6.35-mm) displacement increment the load was held for approximately 2 minutes to observe the reduction in longitudinal force against the backwall as a function of time. On average, the reduction in force after 2 minutes was 7.6%.

A plot of the total load and corresponding baseline curve for the 0° skew test is shown in Figure 6. The resistance of the pile cap in the longitudinal direction is made up of both the passive and shear resistance of the pile cap. This resistance is represented by the difference between the total and baseline curves.

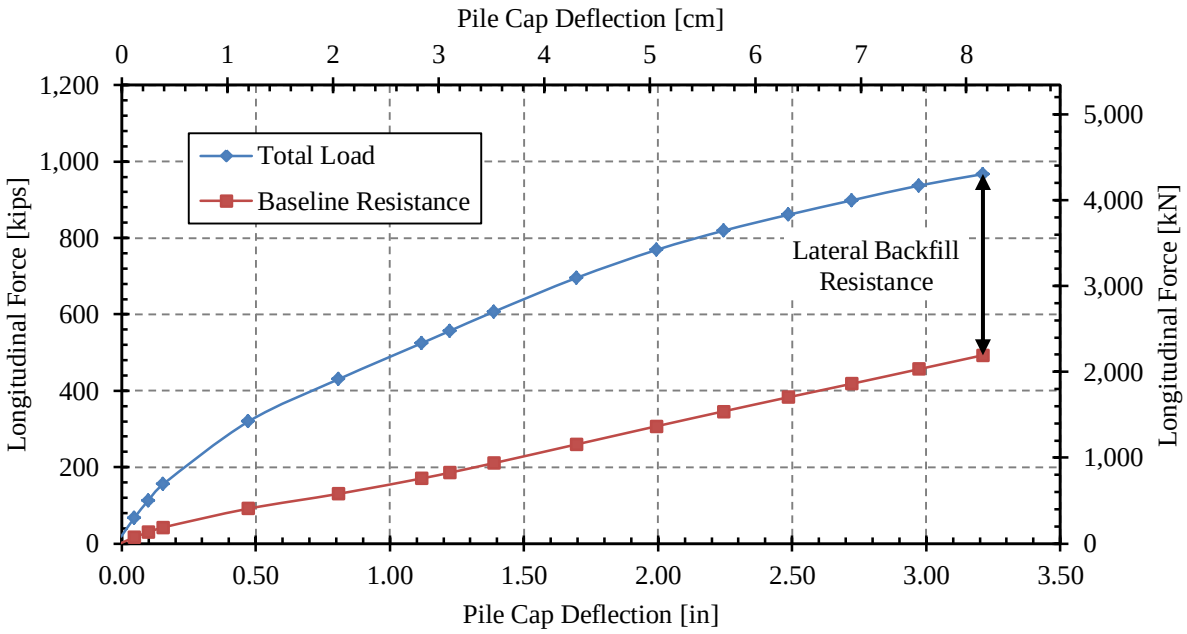

FIGURE 6 Total load and baseline resistance for 0° skew test.

TEST RESULTS

Passive Force-Deflection Curves

Figure 7 shows the passive force verses longitudinal deflection curves for the 0°, 15°, and 30° skew field tests. Passive force was calculated from the total actuator load corrected for the appropriate baseline curve using Equation (2). Backwall deflection was computed as the average deflection of the four string pots on the back of the pile cap. For all three tests, the peak passive force was obtained at normalized deflections between 0.03H and 0.04H which is in good agreement with previous full-scale passive force tests on dense backfill materials (Rollins and Cole 2006). For the 0° skew tests the passive force-displacement curve remained essentially constant beyond the peak, while the passive force decreased about 9% for the 15° skew and 11% for the 30° skew. The backfill for the 15° and 30° skew tests was somewhat denser than for the 0° skew test and thus somewhat more likely to dilate during shearing. As shown in Figure 7 as the skew angle increases the peak passive force decreases.

Figure 8 compares normalized passive force-displacement curves for the field tests conducted in this study and the lab tests conducted by Rollins and Jessee (2012). In this plot, passive force is normalized to the projected backwall area [e.g. 5.5 ft (1.68 m) by 11 ft (3.35 m) rather than 5.5 ft (1.68 m) by 12.7 ft (3.87 m)], and displacement is normalized to backwall height to facilitate the comparison between the field and lab tests.

As the lab tests were conducted so as to simulate plane-strain conditions, and the field tests used an unconfined geometry, the higher normalized passive force for the lab tests is not surprising because the friction angle is normally higher for plane strain conditions. Furthermore, the soil for the lab tests was compacted to a higher relative density. In addition to the higher normalized peak passive force for the 0°, 15° and 30° skew field tests, the peak passive force for the field tests developed at longitudinal deflections between 3% and 4.5% of the backwall height (H) whereas the plane-strain tests developed the peak passive force at deflections between 2% and 3% of the backwall height. The greater drop in passive force after the peak for the lab tests is consistent with the fact that the lab tests were compacted to a denser state and would therefore have had a greater tendency to dilate and experience a decrease in

strength during shearing. The denser state may explain the somewhat more brittle behavior for the lab tests as well.

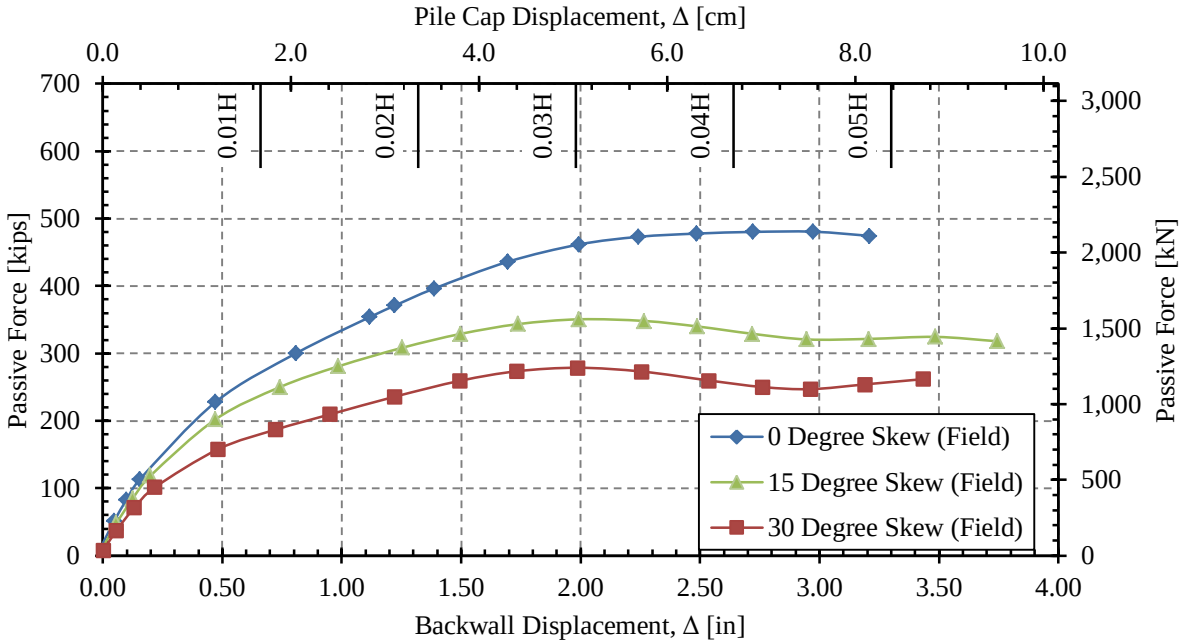

FIGURE 7 Passive force versus longitudinal deflection curves for 0° and 30° skew angles.

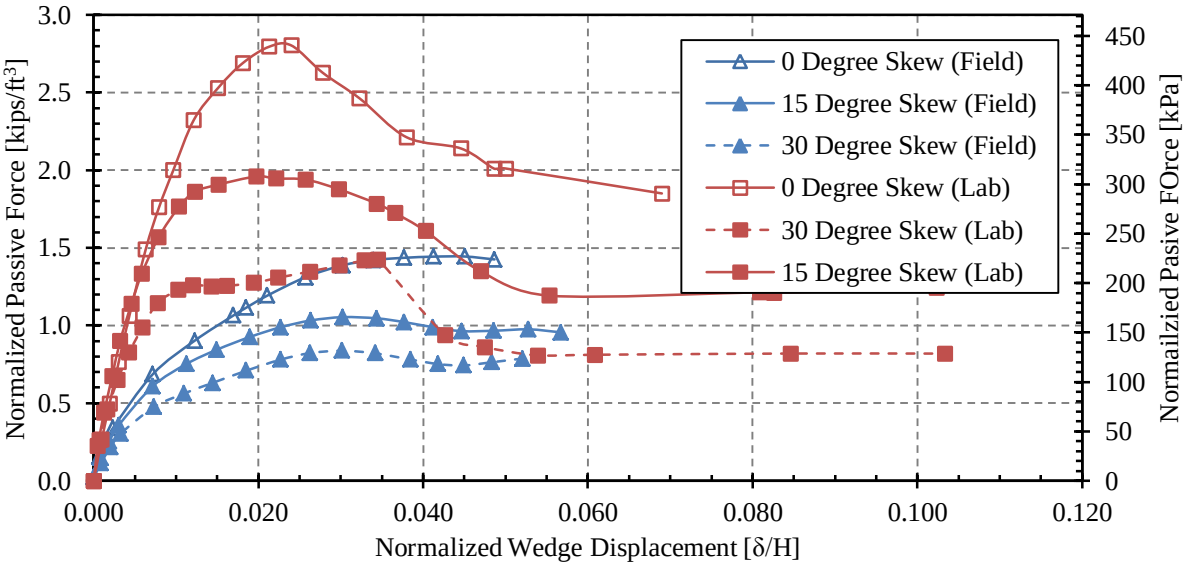

FIGURE 8 Passive force-deflection curves for field and lab tests with passive force normalized to projected with of the backwall multiplied by the backwall height squared versus backwall deflection normalized to backwall height.

Figure 9 plots the passive force reduction factor versus skew angle for the lab tests conducted by Rollins and Jessee (2012), for the numerical models reported by by Shamsabadi et al. (2006), and for the results of this study. As can be seen from the Figure 9, Equation (1) predicts that at skew angles of 15° and 30° the passive force reduction factors should be 75% and 50%, respectively, when compared to the 0° skew case. The measured reduction factors from the field tests were actually 73% and 57% for the 15° and 30° skew tests, respectively. The general agreement between the field test results and the numerical and lab test results suggests that 3D effects and backfill heights may have only a small effect on the reduction in passive force with respect to skew angle as predicted by Equation (1). These results support the notion that the equation for a reduction factor with respect to skew angle is generally applicable. However, additional large scale tests, lab tests and/or numerical analyses should be performed with different abutment geometries and soil types to further substantiate this contention.

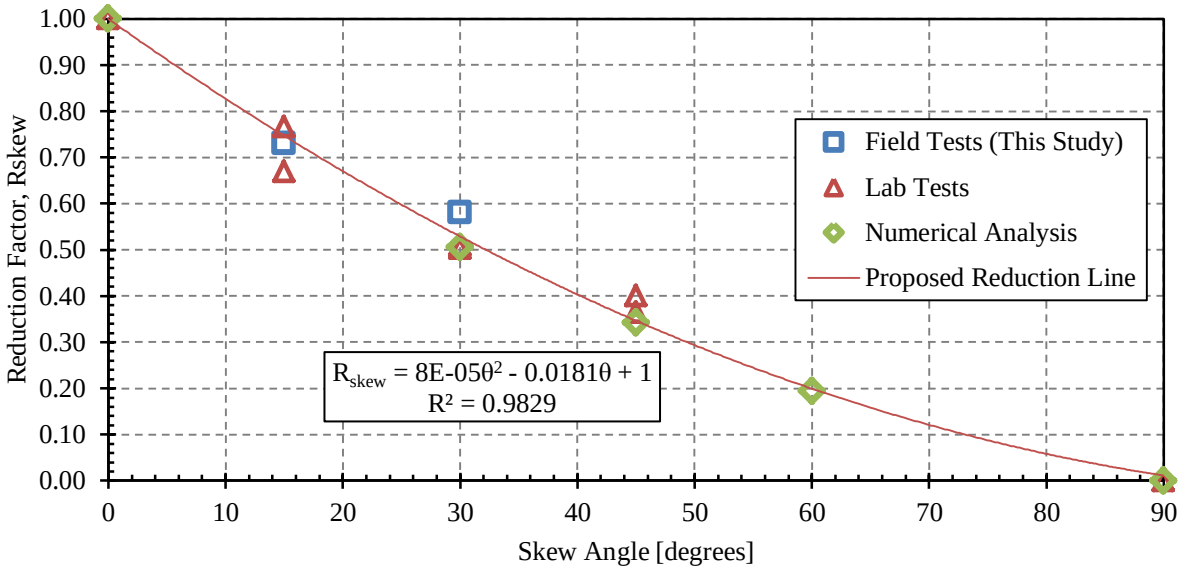

FIGURE 9 Reduction factor, R_{skew} (passive force for a given skew angle normalized by passive force with no skew) plotted versus skew angle based on lab tests (Rollins and Jessee 2012), numerical analyses (Shamsabadi et al. 2006) and s results from field tests in this study.

Pile Cap Displacement vs. Depth

Figure 10 provides longitudinal deflection versus depth profiles obtained from both an inclinometer and a shape accelerometer array for the 15º skew test. Both profiles represent pile cap behavior for the final longitudinal displacement of the test. The depths are referenced to the top of the cap. The average deflection measured by the string pots at two elevations on the pile cap are also shown in Figure 10 for comparison purposes. The graph demonstrates that the measurements for the three systems were reasonably accurate and aligned with each other. The percent difference between the inclinometer and shape array profiles from the top of the cap to a depth of 20 ft (6 m) ranges between 0.1 and 5.2% with an average less than 1%. The dispalacements below a depth of 20 ft (6 m) are very small and the error values in this zone are not particularly meaningful. Similar good agreement was obtained between the shape array and inclinometer for the other tests.

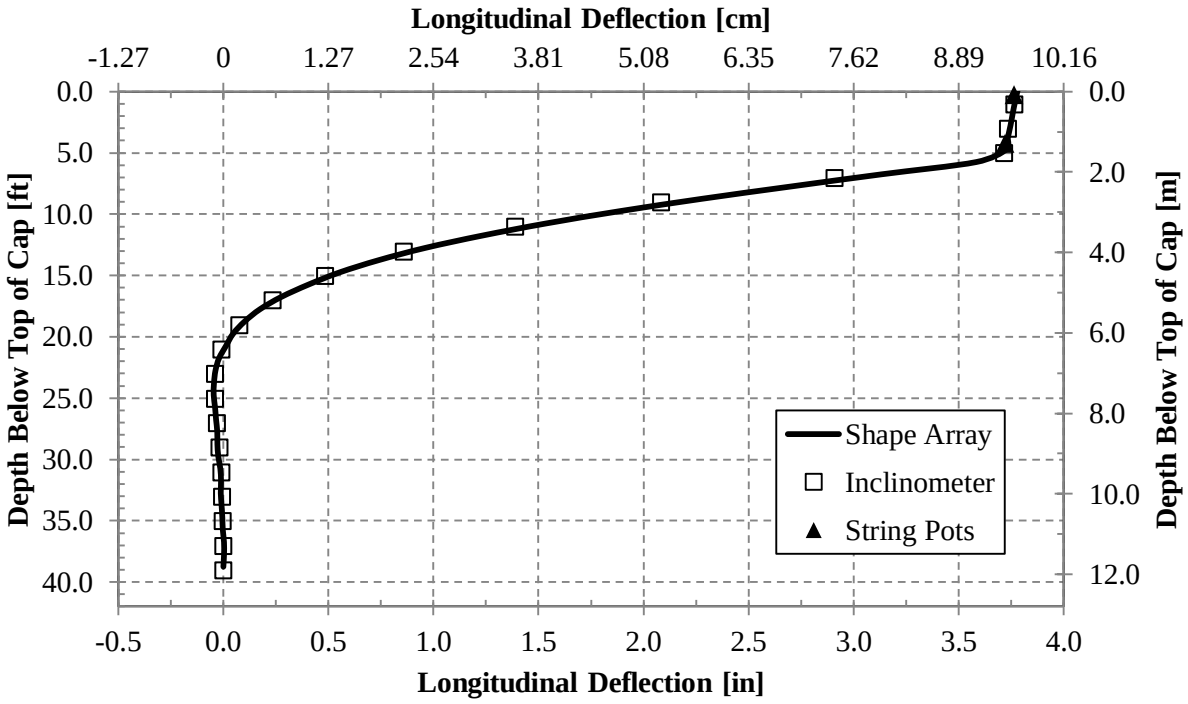

FIGURE 10 North 5.5-ft backfill 15° skew final deflection; comparing inclinometer, shape array and string potentiometers

The measurements indicate a relatively liner deflection profile within the pile cap and small cap rotations. Below the base of the cap, the piles deflect in a non-linear fashion with the deflections reaching a point of counterflexture at depth of approximately 21 ft (6.3 m) and a point of fixity at about 31 ft (9.45 m). Agreement between the north and south inclinometers was generally very good.

Transverse deflection versus depth profiles for the pile cap, recorded by shape array, inclinometer, and LVDTs, are also plotted in Figure 11. Plotted on a smaller scale, the percent error seems larger than the longitudinal error although the magnitude difference is small. However, as observed for the deflections below 20 ft (6 m) in the longitudinal test, the percent difference is exaggerated due to the smaller scale. The percent difference is within the error thresholds of each instrument ($\pm$1.5 mm/30 m for shape array, and $\pm$1.24 mm/30m for inclinometer (Rollins et al. 2009). Error relative to the transverse LVDTs is due to the lower LVDT being only relatively fixed, and therefore moving with the soil near the pile cap, resulting in inaccurate lateral deflection at the bottom of the pile cap. Results are similar for the tests at other skew angles. Once again, the shape of the deflection profile indicates essentially linear deflection in the pile cap and very small rotations. The deflection in the piles is non-linear and decreases to zero at a deflection of about 20 ft (6 m).

Although the inclinometer readings were only taken at the maximum deflection for each load test, shape array profiles in the longitudinal and transverse directions were obtained at each deflection increment for each test. For example, Figure 12 shows profiles of longitudinal deflection vs. depth for each deflection increment. As the deflection level increases the deflection of the pile cap remains linear but the rotation progressively increases while the depth to the point of fixity increases. Similar curves were obtained in the transverse direction. At

smaller deflection levels there are some variations associated with the small measurement errors; however at larger deflections, the data was accurate and useful in visualizing the pile movement.

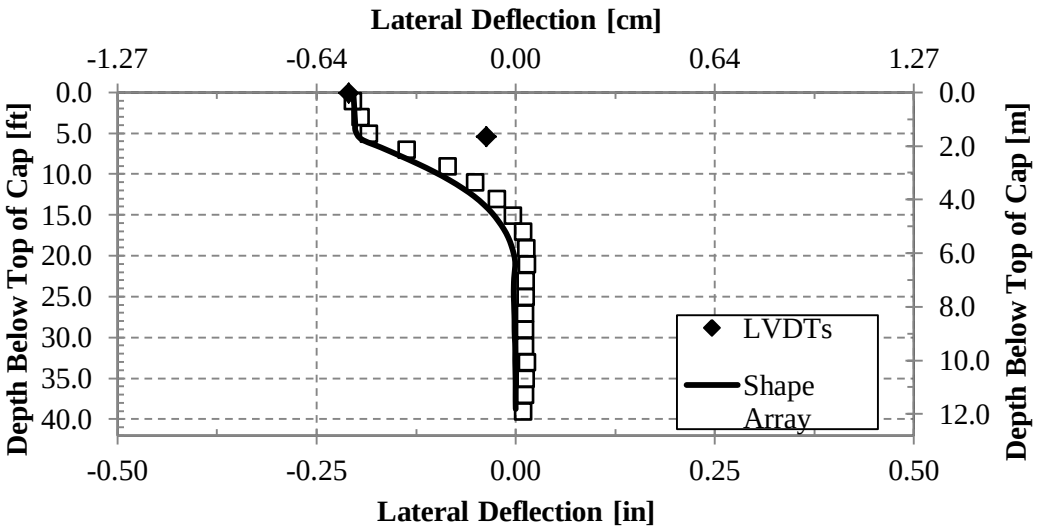

FIGURE 11 North 5.5-ft backfill 15° skew final deflections; comparing inclinometer, shape array and LVDTs

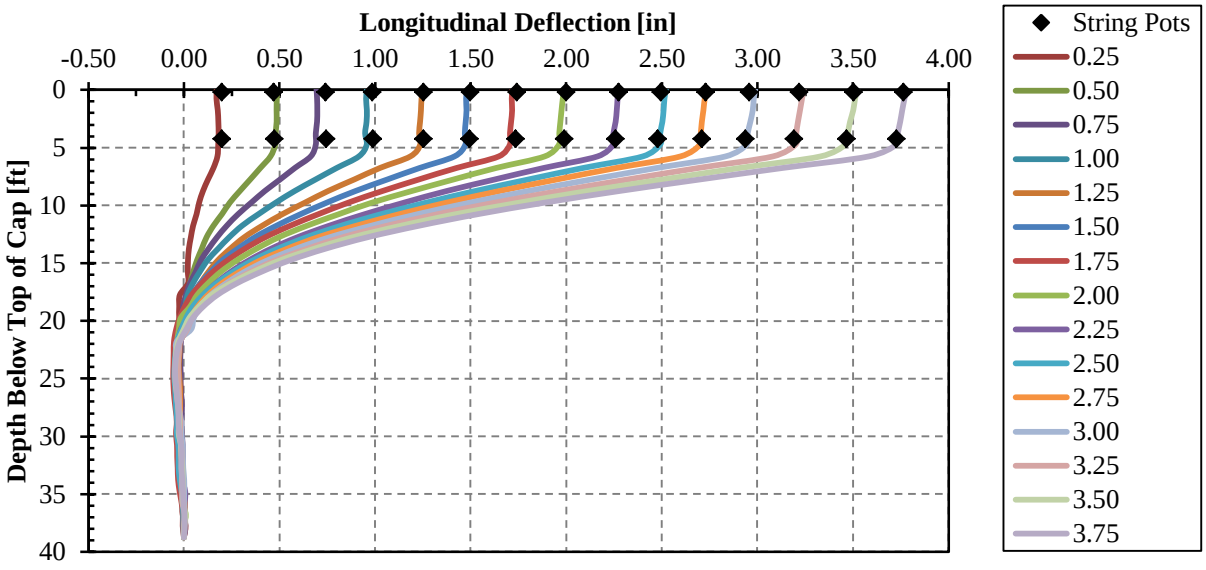

FIGURE 12 Longitudinal deflection vs. depth curves from SAA data at various deflection increments for 15° skew Test

As noted previously, the inclinometer and shape arrays measured transverse deflections for the north and south sides of the pile cap with depth. The measured transverse deflections at the top of pile cap on both the north and south sides of the cap after the last deflection increment for each test are plotted in Figure 13 from a plan view perspective. By connecting these points on the north and south sides, the rotation of the cap can be visualized. Although deflections of both actuators were kept relatively constant throughout the test, rotation and transverse deflection were still affected by the skew angle. As seen in Figure 13, the 0° skew test remained on its initial axis and rotated counter-clockwise by approximately 0.04°. For both the 15° and 30° skews the pile cap ultimately shifted to the left (the direction of the skew) by approximately 0.22 and 0.32 inch, respectively but rotated in opposite directions of approximately 0.03° and 0.02°, respectively. The clockwise rotation for the 15° skew test was most likely attributed to the constraint of the actuators on the pile cap.

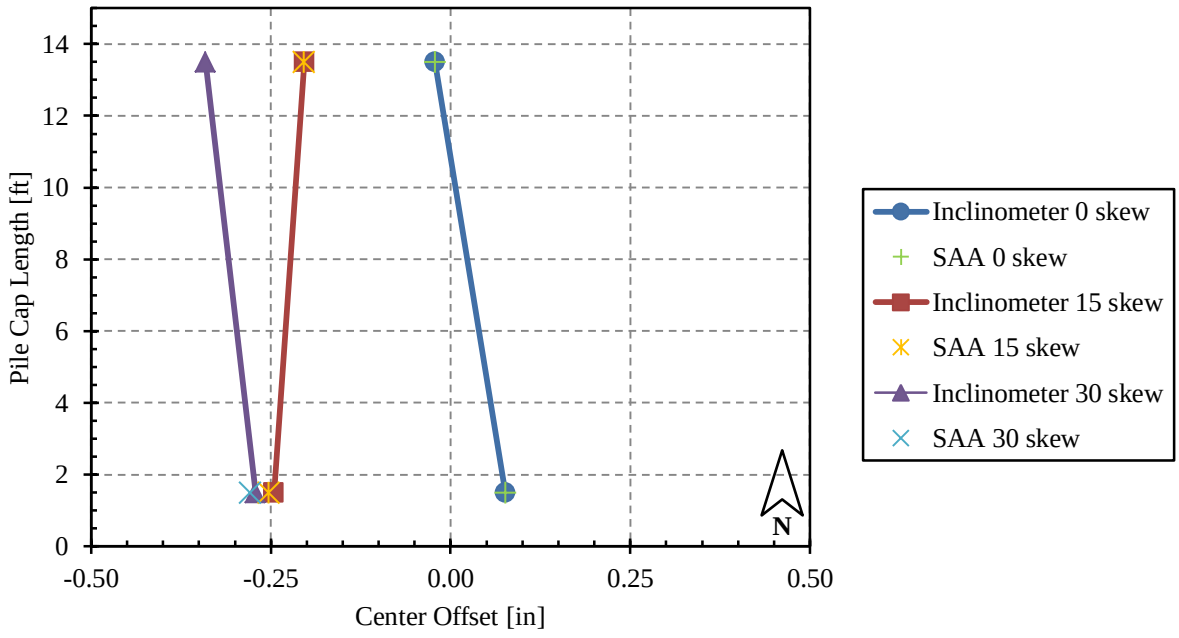

FIGURE 13 Transverse pile cap deflection and rotation determined between north and south shape array and inclinometer data

Pressure Distribution

Figure 14 shows the measured pressure distribution across the width of the pile cap for a series of pile cap displacement increments. Results are plotted from a plan view standpoint relative to the pile cap as illustrated in Figure 4. Analysis of results reveals that the pressure was relatively uniform across the wall face for the first inch of displacement (Figure 14 A &B). At higher displacements, the pressure then increased somewhat at the obtuse (right) end of the pile cap relative to the middle and left portions of the pile cap (Figure 14 C). As the passive force reached a maximum and the soil sheared, the pressure distribution became more triangular (Figure 14 D). The maximum values were measured on the obtuse end of the pile cap at a displacement of 2.5 inches. As the cap continued to move forward, the new pressure distribution remained relatively consistent, finishing with the highest pressure on the obtuse corner, the lowest pressure in the center of the pile cap (Figure 13 E), and a somewhat higher value on acute side. The complete pressure distribution progression can be seen in Figure 13 F.

Results from this test generally agree with findings obtained by Sandford and Elgaaly (1993) in which the pressure on the obtuse side of a fully functioning bridge abutment was significantly greater than on the acute side (see Figure 15). The higher pressures that developed on the obtuse side were attributed to rotation of the abutment that was predicted to have occurred. However, the pressure distribution results from these large-scale tests vary from Sanford's on the acute side of the pile cap where pressures were predicted to be the smallest but were actually much greater than in the middle of the pile cap. It should be noted; however, that Stanford only measured pressure at two points, thus the complete pressure distribution is not accurately known.

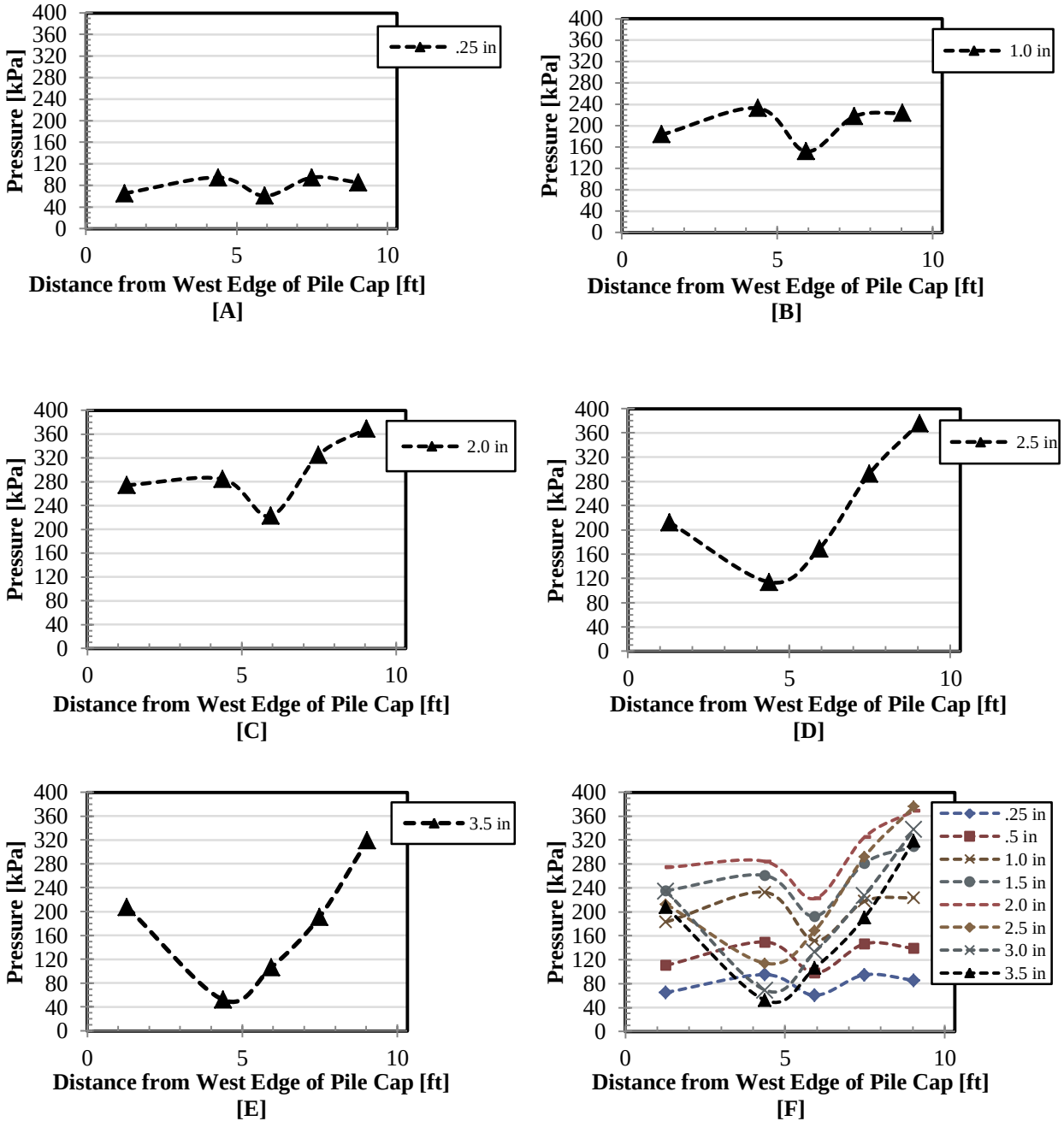

FIGURE 14 Progression of horizontal pressure distribution with pile cap movement

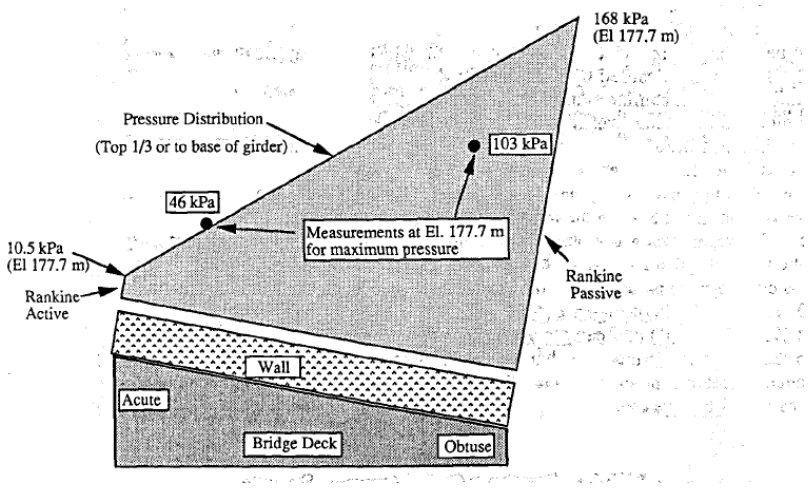

FIGURE 15 Design lateral pressure distribution for skewed abutments (Sandford and Elgaaly 1993)

Although findings from displacement instrumentation reveal that the pile cap rotated slightly counterclockwise and displaced to the left, rotation of the pile cap was greatly restricted by the actuators and underlying piles. By significantly reducing this parameter, it can be implied that rotation is not the only cause of a variance in pressure distribution. Results from this study reveal that higher pressures can still develop on the obtuse side of the cap even if the pile cap is restrained and rotation is relatively small.

Applied Shear Force vs. Transverse Displacement

The relationship between the applied shear force (P_T) and transverse displacement is plotted in Figure 16. The applied shear force was computed using Equation (4) and displacement values were based on shape array measurements taken during testing.

Due to the sharper angle of the 30° skew, the shear force was greater than that on the 15° skew (Figure 16 A) despite the fact that the longitudinal force was greater for the 15° skew than for the 30° skew. The higher shear force also results in greater transverse movements towards the acute side of the pile cap as the skew angle increased. In Figure 16 B the shear force for each cap has been normalized by the maximum shear force. For the 30° skew test the maximum shear force require twice as much movement to develop as for the 15° skew test. The maximum shear force occurred at the maximum

longitudinal force. Once this resistance was reached, transverse movement occurred more freely, resulting in the flatter portions of the lines seen in Figure 16 A and B above.

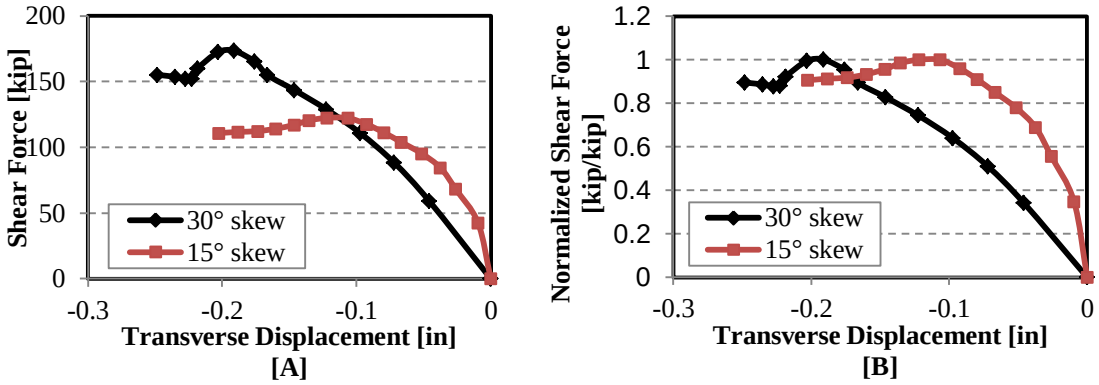

FIGURE 16 [A] Applied shear force versus transverse displacement; [B] Normalized applied shear force versus transverse displacement

According to Duncan and Mokwa (2001), the amount of movement required to mobilize skin friction on an interface is typically between 0.10 and 0.25 inch. Therefore, the applied shear force could be less than the shear resistance (P_R) provided by the abutment wall. In a subsequent report the shear resistance will be calculated once the interface friction angle and cohesion on the pile cap have been more accurately assessed.

Failure Surface Geometry

Plots of the heave contours and surface cracks at the completion of the 0°, 15° and 30° skew tests are shown in Figure 17, Figure 18, and Figure 19, respectively. Heave measurements taken for the 0° skew test show that the maximum heave of 1.97 in (50 mm) occurred near the corners of the pile cap. Maximum heave for the 30° skew test occurred at the acute corner of the cap (west side) and was 2.17 in (55 mm). In both cases, maximum heave was approximately 3% of the maximum height of the failure wedge [5.5 ft (1.68 m)] though heave was less uniform for the 30° skew test.

The maximum measured vertical heave for the 15° skew test of was 3.60 in (91.4 mm) at a longitudinal deflection of 3.75 in (95.3 mm). Significant vertical heave was located along the entire length of the backwall face; however, the largest heave magnitudes were concentrated near the acute corner of

the wedge as observed in the other skew tests. This heave was approximately 6% of the maximum height of the failure wedge [5.5 ft (1.68 m)]. Although vertical heave observed for the 15° skew test is significantly larger than that observed for both the 0° and 30° skew tests, it is highly skewed by a few large values. On average, heave along the backwall face was found to be 2.89 in (73.4 mm) or 4.3%. This significantly higher vertical heave for the 15° skew test is largely attributable to compression of the backfill material directly adjacent to the backwall face, not the passive failure wedge. In addition, the ground in this test was displaced longitudinally farther than the other two tests (3.75 in. versus 3.25 in for the 0° skew and 3.4 in. for the 30° skew).

Because of the transverse wingwalls, the failure surface in all three cases was able to extend between 4 and 5 ft (1.22 and 1.52 m) beyond the edges of the pile cap, thereby increasing the effective width of the failure wedge for all three skew angles. Both the heave pattern and the crack surfaces clearly show the 3D geometry of the developed failure wedge. The transverse movement of the backfill was not measured.

Plots showing the observed and approximate location of the internal shear planes and heave values on cross sections through the sand columns for the 0°, 15° and 30° skew tests are presented in Figure 20, Figure 21, and Figure 22, respectively. As can be seen in Figure 19, surface cracks identifying the failure surface typically occurred at approximately 0.4 to 0.6 in (10 to 15 mm) of heave. Though the complete failure geometry was not observed at the surface of the backfill for the 0° or 15° tests, by extrapolating the shear plane observed in the red sand columns to the surface where approximately 0.4 in (12 mm) of heave occurred, a reasonable location of the potential surface crack could be obtained

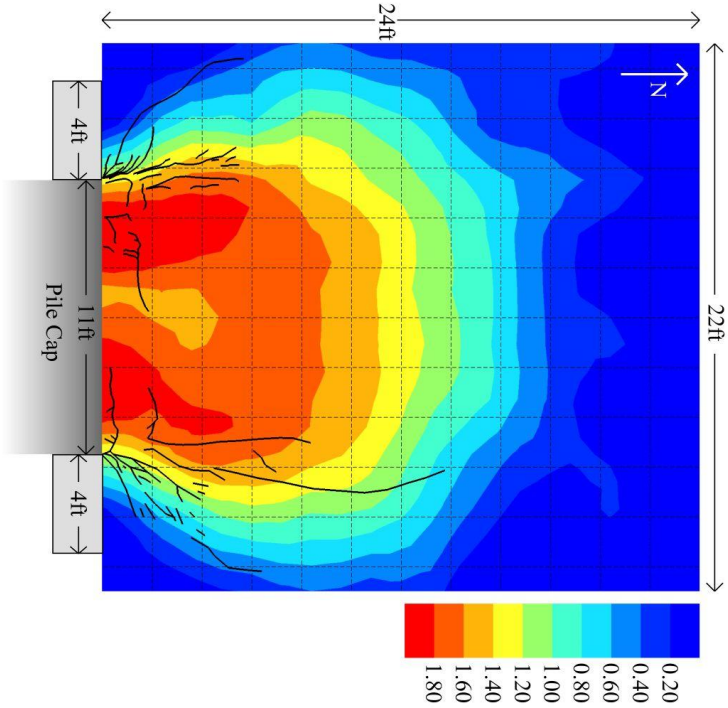

FIGURE 17 Heave contours (units in inches) and surface cracks at 3.21 in (8.15 cm) of longitudinal displacement (test completion) for 0° skew test (NOTE: 1 inch = 2.54 centimeters).

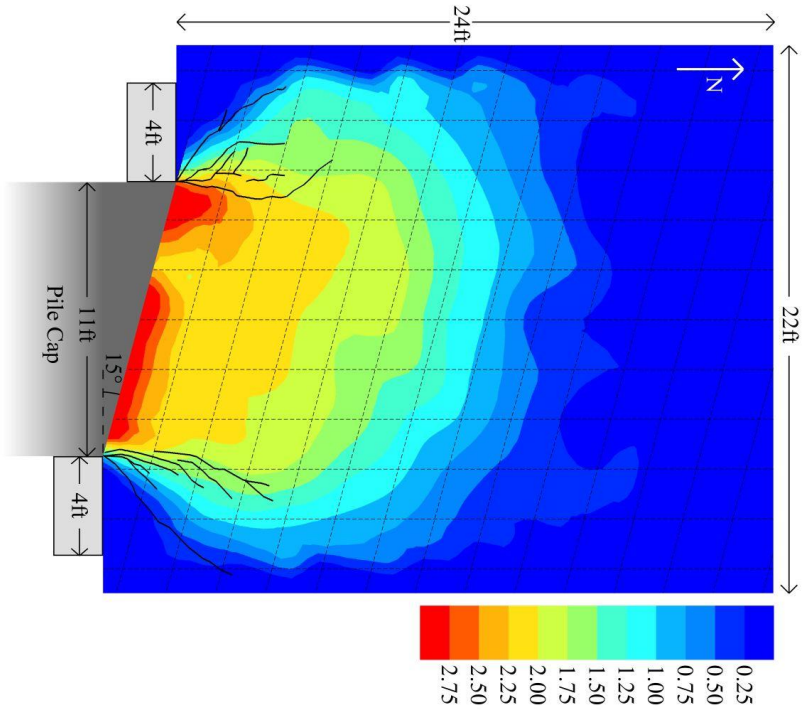

FIGURE 18 Heave contours (units in inches) and surface cracks at 3.75 in (9.53 cm) of longitudinal displacement (test completion) for 15° skew (NOTE 1 inch = 2.54 centimeters)

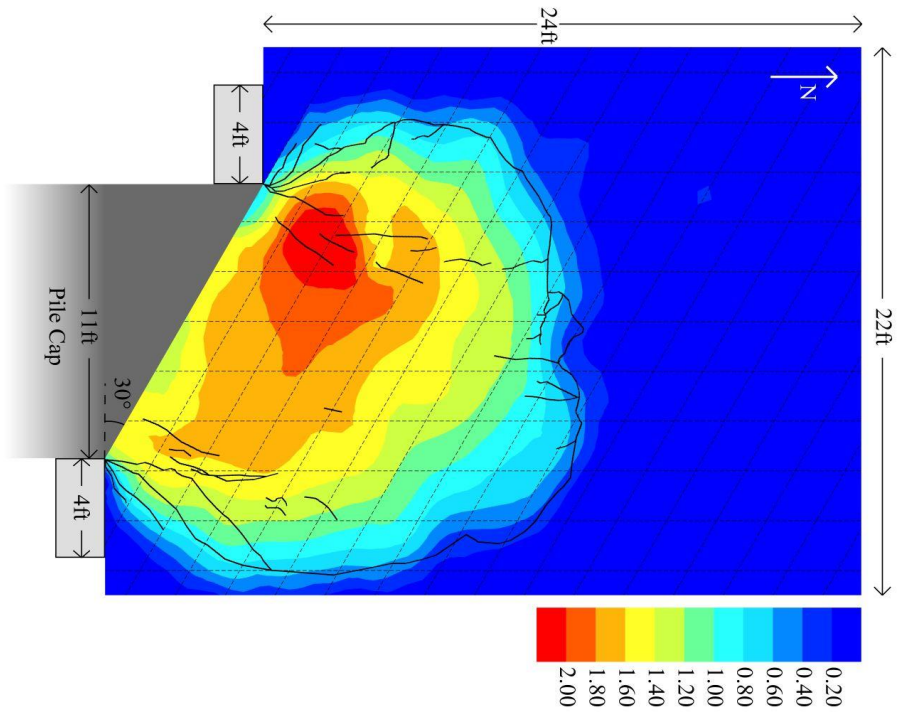

FIGURE 19 Heave contours (units in inches) and surface cracks at 3.43 in (8.71 cm) of longitudinal push (test completion) for 30° skew (NOTE: 1 inch = 2.54 centimeters)

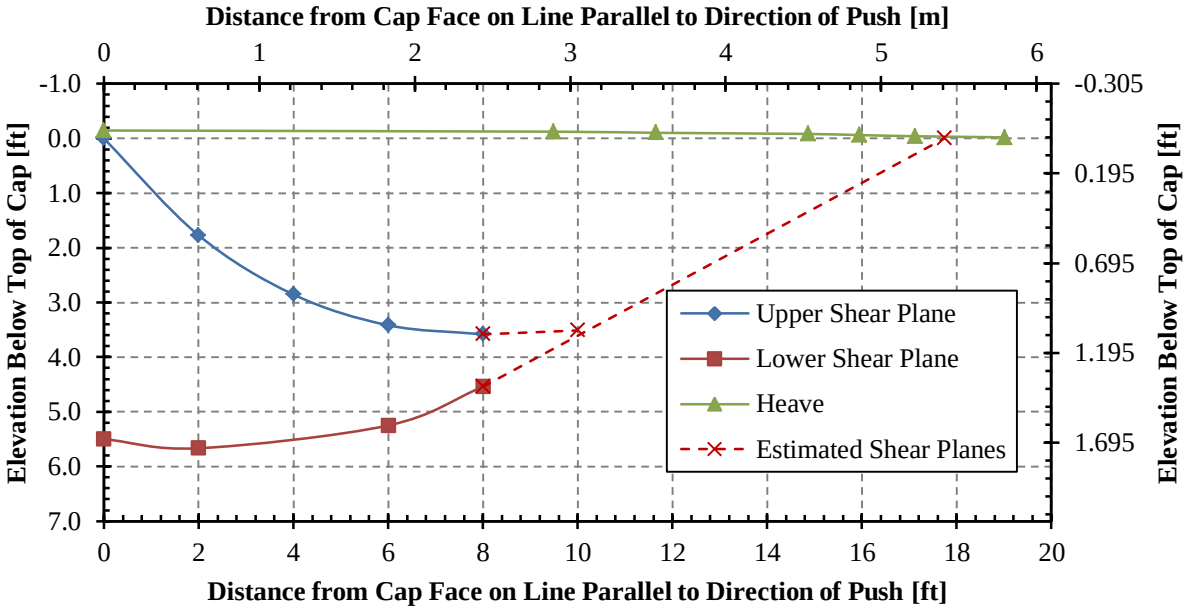

FIGURE 20 Shear plane geometry and ground surface heave for 0° skew test (estimated failure line based on recorded heave measurements).

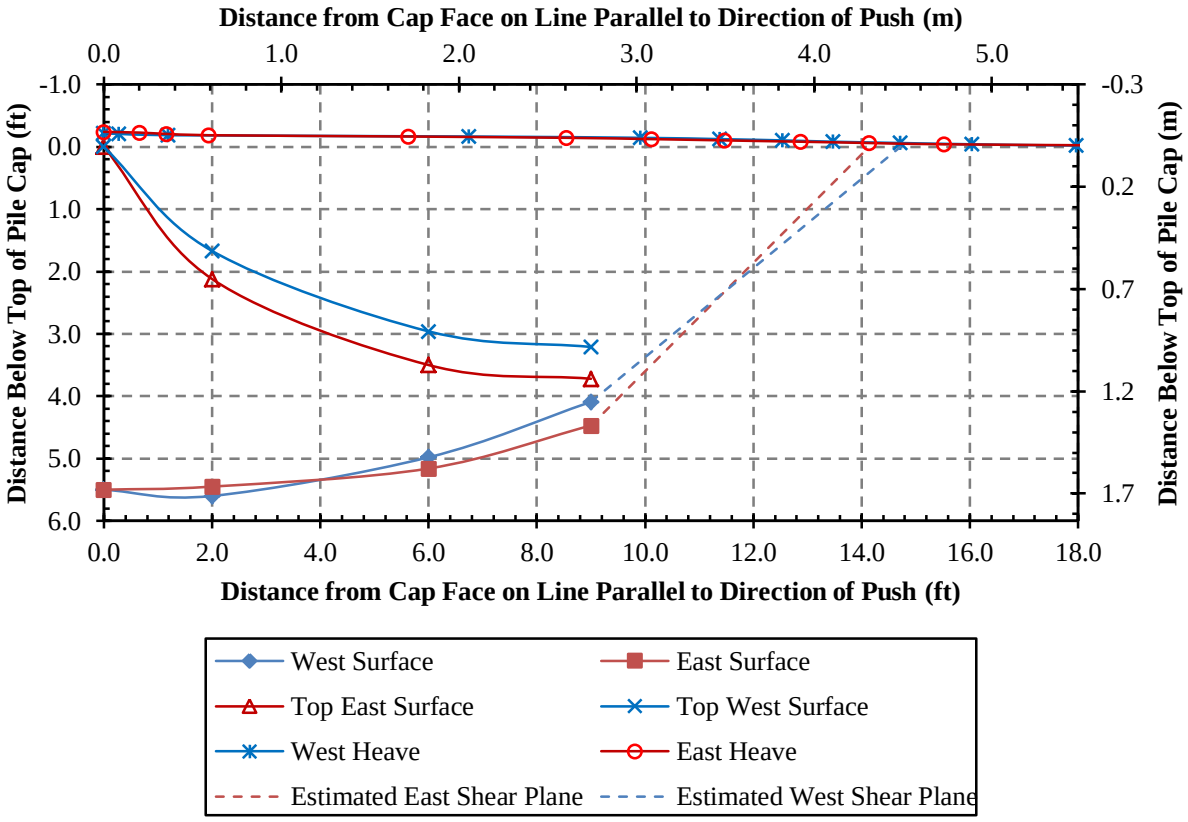

FIGURE 21 Shear plane geometry and ground surface heave for 15° skew test (estimated failure line based on recorded heave measurements)

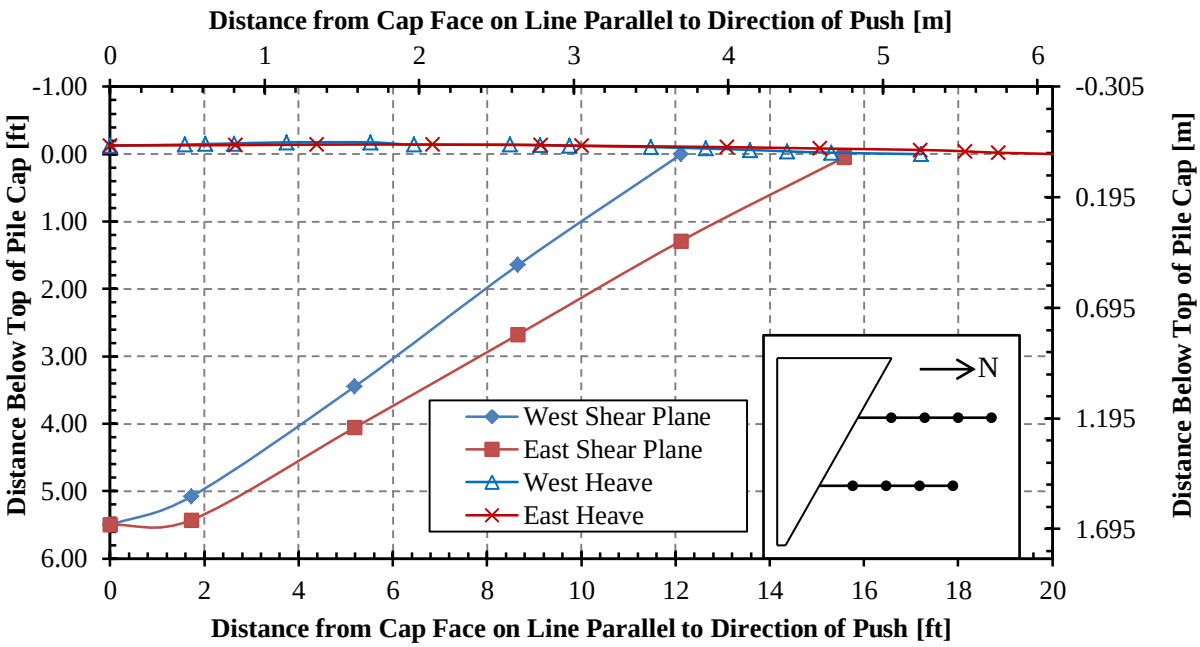

FIGURE 22 East and west shear planes and ground surface heave geometries for 30° skew test; inset shows plan view with approximate locations of red soil columns.

As can be seen from Figure 20, the 0° test failed in a typical log-spiral fashion. In addition to the lower log-spiral shear plane, a second shear plane was observed that originated at the top of the pile cap and then progressed down to intersect the lower shear plane approximately 3.51 ft (1.07 m) below the surface of the pile cap and 10 ft (3.05 m) from the face of the pile cap. The failure surface for the 15° skew test shown in Figure 21 also displayed a failure surface geometry similar to the 0° test. In contrast, the 30° skew test, exhibited failure geometries more consistent with that predicted by the Rankine passive pressure theory than by the log-spiral failure method.

The failure surfaces intercepted the ground surface at approximately 17.7 ft (5.39 m), 17.3 ft (5.3 m) and 16 ft (4.88m) behind the wall for the 0°, 15° and 30° skew tests, respectively, measured in the longitudinal direction. The average angle of inclination of the linear portion of the failure surfaces for the 0° skew test was 30°. Assuming the relationship between friction angle and the angle of inclination (α) of the failure surface shown in Equation (8), the approximate friction angle for the 0° skew tests would be 40°. This value is reasonably consistent with the friction angle determined by the direct shear test.

$$\alpha = 45 - \phi'/2 \quad (8)$$

The 30° skew test, however, exhibited more interesting failure geometry. If distances from the soil columns to the surface cracks were measured parallel to cap movement, the average back-calculated friction angle using Equation (8) was 48°; however if the distances between soil columns and surface cracks were measured perpendicular to the face of the pile cap, the average back-calculated friction angle was 43°. Based on the heave contours and crack patterns in Figure 19, failure perpendicular to the cap seems the most reasonable and gives much better agreement with the friction angle from the zero skew test.

As a result of observations made during the 30° skew test, sand columns were placed in two lines, perpendicular to the backwall face for the 15° test. Figure 21 shows a much better correlation between the east and west failure surfaces than results reported for the 30° skew test as a result of the perpendicular placement of the sand columns. Once again, the failure surface had to be estimated based on the 0.4-in (10 mm) heave contour (Figure 20).

The failure surface for the 15° skew test extended approximately 15 ft (4.57 m) into the backfill measured perpendicularly from the backwall face. The failure surface does not exhibit a purely log spiral or Rankine failure behavior. Instead, the failure surface appears to be a combination of the two. Based on the slope of the linear portion of the curve the back-calculated friction angle would be 38°. As with the 0° skew test, a secondary shear plane was also observed extending from the top of the pile cap until it intersected the bottom failure plane about 9 ft (2.74 m) from the backwall face and at a depth of 4 ft (1.22 m) from the top of the pile cap.

CONCLUSIONS

1. Field tests conducted in this investigation confirm results from lab tests and numerical analyses that there is a significant reduction in peak passive force as abutment skew angle increases.
2. Data obtained from the field tests verify the reduction factor versus skew equation proposed by previous researchers (Rollins and Jessee 2012) despite the differences in backfill thickness [5.5 ft vs. 2.0 ft (1.68 m vs. 0.61 m)], backfill geometry (2D or plane-strain backfill conditions versus 3D or unconfined backfill geometry) and friction angle (ϕ=42° vs ϕ=46°).
3. Despite the variation in skew angle, the peak passive force occurred at longitudinal deflections between 3% and 4.5% of the backwall height for the 0°, 15, and 30° skew case. This value is consistent with results from other large non-skew passive force tests (Rollins and Sparks 2002), but is slightly higher than that reported by Rollins and Jessee (2012) for laboratory skew tests.
4. Although the skew angle varied, the general shape of the failure surface geometry and the resulting overall heave patterns were quite similar for both the 0°, 15°, and 30° tests with the failure surface extending about 4 ft to 5 ft (1.22 m to 1.52 m) past the sides of the pile cap and 16 ft to 17 ft (4.88 m to 5.18 m) from the face of the cap.
5. Applied shear force on the backwall increased as the skew angle increased despite the fact that the longitudinal force decreased. Increased shear force led to greater transverse displacements of the pile cap even with the lateral restraint provided by the piles. Transverse deflections were sufficient to mobilize the skin friction (0.25 inch) on the back of the wall.
6. Measured earth pressures along the length of the backwall for the 30º skew were initially relatively uniform at small longitudinal deflections. As deflections increased, the pressure distribution became more triangular with higher pressures on the obtuse end of the cap.

ACKNOWLEDGMENTS

Funding for this study was provided by an FHWA pooled fund study supported by Departments of Transportation from the states of California, Minnesota, Montana, New York, Oregon, and Utah. Utah served as the lead agency with David Stevens as the project manager. This support is gratefully acknowledged; however, the opinions, conclusions and recommendations in this paper do not necessarily represent those of the sponsoring organizations. We also express appreciation to the Salt Lake City Airport Department for providing access to the test site used in this study.

REFERENCES

AASHTO (2011). "Guide Specifications for LRFD Seismic Bridge Design." 5th Edition, 3-106.

Apirakyorapinit, P., Mohammadi, J., and Shen, J. (2012). "Analytical Investigation of Potential Seismic Damage to a Skewed Bridge." *Practice Periodical on Structural Design and Construction*, 16(1), 5-12.

Burke Jr., M. P. (1994). "Semi-Integral Bridges: Movements and Forces." 1-7.

Caltrans (2001). "Seismic Design Criteria Version 1.2." California Department of Transportation, Sacramento, California.

Duncan, J. M., and Mokwa, R. L. (2001). "Passive Earth Pressures: Theories and Tests." *Journal of Geotechnical and Geoenvironmental Engineering, ASCE*, 127(3), 248-257.

Elnashai, A. S., Gencturk, B., Kwon, O., Al-Qadi, I. L., Hashash, Y., Roesler, J. R., Kim, S. J., Jeong, S., Dukes, J., and Valdivia, A. (2010). "The Maule (Chile) Earthquake of February 27, 2010: Consequence Assessment and Case Studies." Department of Civil and Environmental Engineering, University of Illinois at Urbana-Champaign, 190.

Lee, K. L., and Singh, A. (1971). "Relative Density and Relative Compaction." *Journal of Soil Mechanics and Foundations Design*, 97(7), 1049-1052.

Mokwa, R. L., and Duncan, J. M. (2001). "Experimental Evaluation of Lateral-Load Resistance of Pile Caps." *Journal of Geotechnical and Geoenvironmental Engineering, ASCE*, 127(2), 185-192.

Rollins, K. M., and Cole, R. T. (2006). "Cyclic Lateral Load Behavior of a Pile Cap and Backfill." *Journal of Geotechnical and Geoenvironmental Engineering, ASCE*, 132(9), 1143-1153.

Rollins, K. M., Gerber, T., Cummins, C., and Herbst, M. (2009). "Monitoring Displacement vs. Depth in Lateral Pile Load Tests with Shape Accelerometer Arrays." *Proceedings of 17th International on Soil Mechanics & Geotechnical Engineering*, 3, 2016-2019.

Rollins, K. M., Gerber, T. M., Cummins, C. R., and Pruett, J. M. (2010). "Dynamic Pressure on Abutments and Pile Caps." *Report No. UT-10.18*, B. Y. University, U. D. o. Transportation, and F. H. Administration, eds., Utah Department of Transportation, 255.

Rollins, K. M., Gerber, T. M., and Heiner, L. (2010). "Passive Force-Deflection Behavior for Abutments with MSE Confined Approach Fills." *Report No. UT-10.15*, Utah Department of Transportation.

Rollins, K. M., and Jessee, S. (2012). "Passive Force-Deflection Curves for Skewed Abutments." *Journal of Bridge Engineering*, ASCE, 17(5).

Rollins, K. M., and Sparks, A. E. (2002). "Lateral Load Capacity of a Full-Scale Fixed-Head Pile Group." *Journal of Geotechnical and Geoenvironmental Engineering, ASCE*, 128(9), 711-723.

Sandford, T. C., and Elgaaly, M. (1993). "Skew Effects on Backfill Pressures at Frame Bridge Abutments." *Transportation Research Record: Journal of the Transportation Research Board*, 1-11.

Shamsabadi, A., Kapuskar, M., and Zand, A. (2006 Published). "Three-Dimensional Nonlinear Finite-Element Soil-Abutment Structure Interaction Model for Skewed Bridges." *Paper presented at 5th National Seismic Conference On Bridges and Highways*, 1-10.

Shamsabadi, A., Rollins, K. M., and Kapaskur, M. (2007). "Nonlinear Soil-Abutment-Bridge Structure Interaction for Seismic Performance-Based Design." *Journal of Geotechnical and Geoenvironmental Engineering, ASCE*, 133(6), 707-720.

Steinberg, E., and Sargand, S. (2010). "Forces in Wingwalls from Thermal Expansion of Skewed Semi-Integral Bridges." *Report No. FHWA/OH-2010/16*, Prepared by Ohio University for Ohio Department of Transportation, Athens, OH, 87.

Strassburg, A. N. (2010). "Influence of Relative Compaction on Passive Resistance of Abutments with Mechanical Stabilized Earth (MSE) Wingwalls." M.S. Thesis, Brigham Young University, Provo, UT.

Unjohn, S. "Repair and Retrofit of Bridges Damaged by the 2010 Chile, Maule Earthquake." *Proc., International Symposium on Engineering Lessons Learned from the 2011 Great East Japan Earthquake*, Tokyo, Japan.